Connecting flying backhauls of unmanned aerial vehicles to enhance vehicular networks with fixed 5G NR infrastructure

Dalia Popescu, Philippe Jacquet, Bernard Mans

Received: 27 April 2022 | Revised: 1 June 2022 | Accepted: 3 June 2022

DOI: 10.1049/smc2.12034

IET Smart Cities

The Institution of Engineering and Technology WILEY

ORIGINAL RESEARCH

Connecting flying backhauls of unmanned aerial vehicles to enhance vehicular networks with fixed 5G NR infrastructure

Dalia Popescu[1] | **Philippe Jacquet**[1] | **Bernard Mans**[2]

[1]INRIA, Saclay, France

[2]Macquarie University, Sydney, New South Wales, Australia

Correspondence

Bernard Mans, Macquarie University, North Ryde, Sydney, NSW 2109, Australia.
Email: bernard.mans@mq.edu.au

Funding information

Australian Research Council, Grant/Award Number: DP170102794

Abstract

This paper investigates moving networks of Unmanned Aerial Vehicles to extend connectivity and guarantee data rates in the 5G by analysing possible hovering locations based on limitations such as flight time and coverage. The authors provide analytic bounds on the requirements in terms of connectivity extension for vehicular networks served by fixed Enhanced Mobile BroadBand infrastructure, where both vehicular networks and infrastructures are modelled using stochastic and fractal geometry as a model for urban environment. The authors prove that assuming n mobile nodes (distributed according to a hyperfractal distribution of dimension d_F) and an average of ρ Next Generation NodeB (gNBs), distributed like a hyperfractal of dimension d_r if $\rho = n^{\theta}$ with $\theta > d_r/4$ and letting n tending to infinity (to reflect megalopolis cities), then the average fraction of mobile nodes not covered by a gNB tends to zero like $O\left(n^{-\frac{(d_F-2)}{d_r}\left(2\theta-\frac{d_r}{2}\right)}\right)$. Interestingly, the authors prove that the average number of drones, needed to connect each mobile node not covered by gNBs, is comparable to the number of isolated mobile nodes. The authors complete the characterisation by proving that when $\theta < d_r/4$ the proportion of covered mobile nodes tends to zero. The authors offer insights on the placement of the 'garage of drones', the home location of these nomadic infrastructure nodes, to minimise the 'flight-to-coverage time'. The authors provide a fast procedure to select the relays that will be garages (and store drones) in order to minimise the number of garages and minimise the delay. The authors' analytical results are confirmed using simulations in Matlab.

KEYWORDS

5G, drone, enhanced mobile BroadBand (eMBB), flying backhaul, mmWave, mobile vehicular network, smart city, UAVs, V2X

1 | INTRODUCTION

1.1 | Mobile networks

5G New Radio (5G NR) is envisioned to offer a diverse palette of services to mobile users and platforms, with often incompatible types of requirements. 5G will support (i) the *enhanced Mobile BroadBand (eMBB)* applications with a throughput of order of 100 Mbit/s per user, (ii) the *Ultra Reliable Low Latency Communications (URLLC)* for industrial and vehicular environments with the hard constraint of 1 ms latency and 99.99% reliability, and (iii) the *massive Machine Type Communications* with a colossal density in order of 100 per square km. 5G will achieve this through a new air interface and novel network architectures that will either be evolved from the current 4G systems or be completely drawn from scratch.

However, it is clear that by the time the 5G standards start to be deployed, many of these important challenges will still remain open and a truly disruptive transition from current 4G systems will only occur over time. One of these challenges is

the ability of the network to adapt efficiently to the evolution of traffic demand in space and time, in particular when new frequency bands are exploited in ranges much higher than ever tried before, for example, Frequency Range (FR) 4 at over 52.6 GHz.A key difference from today's 4G systems is that 5G networks will be characterised by a massive density of nodes, both human-held and machine-type: according to the Ericsson mobility report (November 2021), 5G subscriptions are forecast to reach 4.4 billion globally by the end of 2027. A larger density of wireless nodes implies a larger standard deviation in the traffic generation process. Network planning done based on average (or peak) traffic predictions as done for previous systems will only be able to bring sub-optimal results. Moreover, the '*verticals*' of major interest identified for 5G networks (automotive, health, fabric-of-the-future, media, and energy) come with rather different requirements and use cases. Future networks will handle extremely heterogeneous traffic scenarios.

To tackle these problems, 5G NR networks are to exhibit a network flexibility that is much higher than in the past: infrastructure nodes must be adaptable enough in order to be able to smoothly and autonomously react to the fast temporal and spatial variations of traffic demand. The level of flexibility that can be achieved through such advances still faces a fundamental limit: the hardware location is static and the offered network capacity and coverage on a local scale is fundamentally limited by the density of infrastructure equipment (radio transceivers) in the area of interest [1].

This opens up the possibility of *Moving Networks*, informally defined as moving nodes, with advanced network capabilities, gathered together to form a movable network that can communicate with its environment. Moving Networks will help 5G systems to become demand-attentive, with a level of network cooperation that will facilitate the provisioning of services to users characterised by high mobility and throughput requirements or in situations where a fixed network cannot satisfy traffic demand. A key player in a moving network is the communication entity with the highest number of degrees of freedom of movement: the drone. Unmanned Aerial Vehicle (UAV) assistance has now developed as a solid paradigm [2].

1.2 | Contributions

In this work we initiate the study and design of moving networks by a first analysis of the provisioning and dimensioning of a network where drones act as flying backhaul. The setup we make use is that of a smart city in which we design one of the complex 5G NR urban scenarios: drones coexist with vehicular networks and fixed telecommunication infrastructures.

Making use of the innovative model called Hyperfractal [3] for representing the traffic density of vehicular devices in an urban scenario and the distribution of static telecommunication infrastructure, we derive the requirements in terms of resources of UAVs for enhancing the coverage required by the users. Informally, we compute the expected percentage of the users in poor coverage conditions and derive the average number of drones necessary for ensuring the coverage with high reliability of the vehicular nodes. Furthermore, we discuss the notion of 'garage of drones', the home location of these nomadic infrastructure nodes, the drones. Our paper provides exact analytic bounds on the requirements in terms of connectivity extension for vehicular networks served by fixed eMBB infrastructure. The analytical results can thus be used to inform the design and implementation of the solutions by identifying what is possible and what is not achievable with the particular features of the urban environment at hand.

More specifically, our contributions are:

- An innovative macro model for urban environment, providing a new perspective on smart cities, where both vehicular networks and fixed eMBB infrastructure networks are modelled using stochastic and fractal geometry (Section 2). The model allows to compute precise bounds on the requirements in term of connectivity, or lack of thereof.
- A proof that the average fraction of mobile nodes not covered by the fixed infrastructure (gNBs) either tends to zero or tends to the actual number of nodes in the network with the characterisation of the exact threshold (Theorem III.1 and Theorem III.2 in Section 3).
- A proof that the number of drones to connect the isolated mobile nodes is asymptotically equivalent to the number of isolated mobile nodes (Theorem III.3 in Section 3), thus proving that, typically, one drone is sufficient to connect an isolated mobile node to the network.
- An introduction and analysis of the 'flight-to-coverage time' for the deployed drones, helping in their optimised placement and recharge in the network (Section 4). We provide a fast procedure to select the relays that will be garages (and store drones) in order to minimise the number of garages and minimise the delay.
- Simulations results in Matlab that confirm our stochastic results (Section 5).

1.3 | Related studies

While their introduction to commercial use has been delayed and restricted to specific use-cases due to the numerous challenges (e.g. Ref. [4]), the flexibility the drones bring to the network planning by their increased degree of movement has motivated the industry to push towards their introduction in wide scenarios of 5G.

We refer the reader to recent relevant surveys on UAV assistance in smart cities (e.g. Ref. [2, 5–7]). A thorough Tutorial on UAV Communications for 5G and Beyond is presented in Ref. [8], where both UAV-assisted wireless communications and cellular-connected UAVs are discussed (with UAVs integrated into the network as new aerial communication platforms and users).

Importantly, many new opportunities have been often highlighted (e.g. in Ref. [9]), including (not exhaustively):

- Coverage and capacity enhancement of beyond 5G wireless cellular networks:
- UAVs as flying base stations for public safety scenarios;
- UAV-assisted terrestrial networks for information dissemination;
- Cache-enabled UAVs;
- UAVs as flying backhaul for terrestrial networks.

Considerations for a multi-UAV enabled wireless communication system, where multiple UAV-mounted aerial base stations are employed to serve a group of users on the ground have been presented in Ref. [10]. Minimising their average energy consumption while providing an efficient coverage strategy has also been considered in Ref. [11]. An overview of UAV-aided wireless communications, introducing the basic networking architecture and main channel characteristics, and highlighting the key design considerations as well as the new opportunities to be exploited is presented in Ref. [12].

Grasping the interest for this new concept of communication, the research community has started analysing the details of the new communication paradigms introduced with the drones. In the beginning, drones have been considered for delivering the capacity required for sporadic peaks of demand, such as in entertainment events, to reach areas where there is no infrastructure or the infrastructure is down due to a natural catastrophe. Yet in the new 5G NR scenarios of communication, drones are not only used in isolated cases but are also considered as active components in the planning of moving networks in order to provide the elasticity and flexibility required by these. In this sense, using drones for the 5G Integrated Access and Backhaul (IAB) ([13, 14]) is one of the most relevant use-case scenarios, ensuring the long-desired flexibility of coverage aimed with an adaptable cost of infrastructure.

The research community has been looking at specific problems in wireless networks employing drones. In Ref. [15], the authors prove the feasibility of multi-tier networks of drones giving some first insight on the dimensioning of such a network. The work done in Ref. [16] uses two approaches, a network-centric approach and a user-centric approach, to find the optimal backhaul placement for the drones. On the other hand, in Ref. [17], the authors propose a heuristic algorithm for the placement of drones. The authors of Ref. [18] analyse the scenario of a bidirectional highway and propose an algorithm for determining the number of drones for satisfying coverage and delay constraints. A delay analysis is performed in Ref. [19] on the same type of scenario. Simplified assumptions are used in Ref. [20] to showcase the considerable improvements brought by UAVs as assistance to cellular networks. The movement of network of drones, so-called swarm is analysed in Ref. [21], and efficient routing techniques are proposed. Drones are so much envisioned for the networks of the future that the authors of Ref. [22] provide solutions for a platform of drones-as-a-service that would answer the future operator demands.

Following these observations from the state of the art, we aim to initiate a complex analysis of the use of the drones in a smart city for different purposes. To our knowledge, this is the first analysis which looks at the entire macro urban model of the city, incorporating both devices and the fixed telecommunications infrastructure. In our analysis, the drones are used as a flying backhaul for extending the coverage to users in poor conditions.

2 | SYSTEM MODEL AND SCENARIO

The communication scenario in our work has the aim to provide a flexible network architecture that allows serving the vehicular devices with tight delay constraints. The scenario comprises three types of communication entities: the vehicles which we denote as the user equipments (UEs), the fixed telecommunication infrastructure called Next Generation NodeB (gNBs) and the moving network nodes which are the drones also called UAVs.

The scenario we tackle in this work is as follows. An urban network of vehicles is served by a fixed telecommunication infrastructure. Due to the limited coverage capability using millimetre wave (mmwave) in urban environments, the costs of installing fixed telecommunication infrastructure throughout the entire city and the mobility of the vehicles in the urban area, some users will be outside of the coverage areas. This is no longer acceptable in 5G as International Mobile Telecommunications Standards (IMT 2020 [23]) require for most of the users and in particular for URLLC users, full coverage and harsh constraints for delay. Unmanned Aerial Vehicles (such as drones) will therefore be dynamically deployed for reaching the so-called 'isolated' users, forming the flying backhaul of the network.

2.1 | Communication model

For the sake of simplicity, we consider the communication to be done in the FR2 (frequency range 2) 28 GHz frequency band using beamforming, mmwave technology in half-duplex mode. This follows the current specifications, yet we foresee the modelling to be easily extended for FR3 (frequency range 3) and FR4 (frequency range 4). This leads to highly directive beams with a narrow aperture, sensitive to blockage and interference. To this end, in our modelling we integrate the *canyon* propagation model [3], which implies that the signal emitted by a mobile node propagates only on the street where it stands on.

We consider that drones, gNBs and UEs use the same frequency band, modulation schemes and transmission power. The relay nodes (gNBs and UAV) are located at medium altitude; thus, the transmissions are in line of sight. This results to the same transmission range, assuming a collision free transmission and same ambient noise everywhere in the city. We denote R_0 in this uniform transmission range; the performance of milimetre radio communication suggest $R = 100$ m.

We model a city like a square of side L_n where n is the number of mobile users. There are many possible growth

function for L_n, but for the remaining of the paper we will use $L_n = L_1\sqrt{n}$. The reasoning behind this choice of transmission range is as follows. The population of a city is proportional to the area of the city; in other words, the densities are similar. Of course this must be understood when cities are in the same cultural areas. It is clear that the cities in China or in Indian areas are more densely populated than the cities in America or in Europe but in the same cultural area they tend to be very similar (e.g. Ref. [24, 25]). The population of cars also follows the population of the city (in fact the local variations of car densities tend to counter the local variation of population densities [26]); therefore, the population of cars is expected to be actually more aligned with the area of the city, area $= A \cdot n$ where A is a constant and thus $L_1 = \sqrt{A}$.

Since the results in this paper mainly depend on the exponent of n, this factor is not significant for the main theorem in the first part of the paper. However, a reasonable assumption is to consider around 1000 mobile nodes per square kilometre, thus $L_1 \approx \sqrt{1000}$ m.

The mobile nodes that we treat in this modelling are vehicular devices or UEs located on streets. These mobile nodes are not significantly moving at packet transmission level because of the expected high bit rate of 5G compared to physical speeds; thus, considering them fixed at a random position is a reasonable assumption in the first part of the paper, which handles coverage statistics and which requires analysis of snapshots of the network at random times. In section 4, we will address the continuity of communication at connection level, and the relative speeds of mobile nodes will be discussed.

The UAV will communicate with the mobile users on the radio access network interface, similar to a gNB to UE exchange. For drone-to-drone communication and drone-to-gNB communication, it is the IAB interface that is used, in the same frequency band.

We consider that for a UE to benefit from the dynamical coverage provided by UAVs, it has to be already registered to the network through a previously performed random access procedure (RACH), and we only treat users in connected mode; therefore, the network is aware about the existence of the UE, its context and service requirements and, when the situation occurs, that it is experiencing a poor coverage.

We assume that the position of a registered UE in connected mode is known to the network and the evolution can be tracked (speed, direction of movement). The position of the UE can be either UE-based positioning or UE-assisted positioning, both allowing enough degree of accuracy for a proactive preparation of resources in the identified target cell. These are assumptions perfectly in line with the objectives of Release 17 of 5G NR.

As a consequence of this knowledge in the network, the gNB that is currently serving the vehicle can inform the target gNB about the upcoming arrival of the vehicle such that the target gNB can prepare/send a drone (if necessary) for ensuring the service continuity to the UE.

The drones will be dynamically deployed in order to extend the coverage of the gNBs towards the UEs, forming a flying backhaul.

2.2 | Hyperfractal modelling for an urban scenario

As 5G is not meant to be designed for a general setup but rather have specific solutions for all the variety of communication scenarios (in particular for *verticals*), the idea of a smart city in which one is capable of translating different parameters and features in order to better calibrate the private network being deployed arises as a possible answer to these stringent requirements.

While urban environments are complex, chaotic, discontinuous and irregular in their superficial physical appearances, there is an obvious similarity in all modern cities. Beneath lies an order that is regular and self-similar, which allows us to define a geometry of this chaos: *a city itself is fractal*. Cities yield excellent examples of fractals [27–30].

A hyperfractal representation of urban settings [3], in particular for mobile vehicles and fixed infrastructures (such as red lights), is an innovative representation that we chose for modelling the UEs and eMBB infrastructures here. With this model, one is capable of taking measurements of vehicular traffic flows, urban characteristics (streets lengths, crossings etc.), fit the data to a hyperfractal with computed parameters and compute metrics of interest. Independently, this is an interesting step towards achieving modelling of smart urban cities that can be exploited in other scenarios.

2.2.1 | Mobile users

The positions of the mobile users and their flows in the urban environment are modelled with the hyperfractal model described in Ref. [3, 31, 32]. In the following, we only provide the necessary and self-sufficient introduction to the model, but a complete and extended description can be found in Ref. [3].

The map model lays in an $L_n \times L_n$ square embedded in the 2-dimensional Euclidean space. The support of the population is a grid of streets. Let us denote this structure by $\mathcal{X} = \bigcup_{\ell=0}^{\infty} \mathcal{X}_\ell$. A street of level H consists of the union of consecutive segments of level H in the same line. The length of a street is the length of the side of the map, namely L_n.

The mobile users are modelled by means of a Poisson point process Φ on $\mathcal{X}$ with total intensity n ($0 < n < \infty$) having 1-dimensional intensity per street unit length

$$\lambda_\ell = \frac{n}{L_n}(p/2)(q/2)^\ell \tag{1}$$

on $\mathcal{X}_\ell$, $\ell = 0, \ldots, \infty$, with $q = 1 - p$ for some parameter p ($0 \le p \le 1$). Note that Φ can be constructed in the following way: one samples the n mobile users such that each mobile is placed independently with probability p on $\mathcal{X}_0$ according to the uniform distribution and with probability $q/4$, it is recursively located in the similar way in one of the four quadrants of $\bigcup_{\ell=1}^{\infty} \mathcal{X}_\ell$.

The intensity measure of Φ on $\mathcal{X}$ is hypothetically reproduced in each of the four quadrants of $\bigcup_{\ell=1}^{\infty}\mathcal{X}_\ell$ with the scaling of its support by the factor half and of its value by $q/4$.

The fractal dimension is a scalar parameter characterising a geometric object with repetitive patterns. It indicates how the volume of the object decreases when submitted to a homothetic scaling. When the object is a convex subset of a Euclidian space of finite dimension, the fractal dimension is equal to this dimension. When the object is a fractal subset of this Euclidian space as defined in Ref. [33], it is possibly a non-integer but positive scalar strictly smaller than the Euclidian dimension. When the object is a measure defined in the Euclidian space, as it is the case in this paper, then the fractal dimension can be strictly larger than the Euclidian dimension. In this case, we say that the measure is *hyperfractal* [34].

Remark 1 The fractal dimension d_F of the intensity measure of Φ satisfies

$$\left(\frac{1}{2}\right)^{d_F} = \frac{q}{4} \qquad \text{thus} \qquad d_F = \frac{\log\left(\frac{4}{q}\right)}{\log 2} \geq 2.$$

Figure 1a shows an example of support iteratively built up to level $H = 3$ while Figure 1b shows the nodes obtained as a Poisson shot on a support of a higher depth, $H = 5$.

2.2.2 | Fixed telecommunication infrastructure, gNBs

We denote the process for gNBs by Ξ. To define Ξ, it is convenient to consider an auxiliary Poisson process Φ_r with both processes supported by a 0-dimensional subset of $\mathcal{X}$, namely the set of intersections of segments constituting $\mathcal{X}$. We assume that Φ_r has Poisson intensity $\rho p(H, V)$ with

$$p(H, V) = (p')^2\left(\frac{1-p'}{2}\right)^{H+V} \tag{2}$$

on all intersections $\mathcal{X}_H \cap \mathcal{X}_V$ for $H, V = 0, \ldots, \infty$ for some parameter p', $0 \leq p' \leq 1$ and $\rho > 0$. That is, on any such intersection, the mass of Φ_r is a Poisson random variable with parameter $\rho p(H, V)$ and ρ is the total expected number of points of Φ_r in the model. The self-similar structure of Φ_r is well explained by its construction in which we first sample the total number of points from a Poisson distribution of intensity ρ and given $\Phi_r(\mathcal{X}) = M$, each point is independently placed with probability $(p')^2$ in the central crossing of $\mathcal{X}_0 \cap \mathcal{X}_0$, with probability $p'\frac{1-p'}{2}$ on some other crossing of one of the four segments forming $\mathcal{X}_0$ (namely on $\bigcup_{V>0}\mathcal{X}_0 \cap \mathcal{X}_V$) and, with the remaining probability $\left(\frac{1-p'}{2}\right)^2$, in a similar way, recursively, on some crossing of one of the four quadrants of $\bigcup_{l=1}^{\infty}\mathcal{X}_l$ (namely on $\bigcup_{H>0,V>0}\mathcal{X}_H \cap \mathcal{X}_V$).

Note that the Poisson process Φ_r is not simple and we define the process Ξ for gNBs as the support measure of Φ_r, that is, only one gNB is installed in every crossing where Φ_r has at least one point.

Remark 2 Note that fixed infrastructure Ξ forms a non-homogeneous binomial point process (i.e. points are placed independently) on the crossings of $\mathcal{X}$ with a given intersection of two segments from $\mathcal{X}_H$ and $\mathcal{X}_V$ occupied by a gNB point with probability $1 - \exp(-\rho p(H, V))$.

Similarly to the process of mobile nodes, we can define the fractal dimension of the gNBs process.

Remark 3 The fractal dimension d_r of the probability density of Ξ is equal to the fractal dimension of the intensity measure of the Poisson process Φ_r and verifies

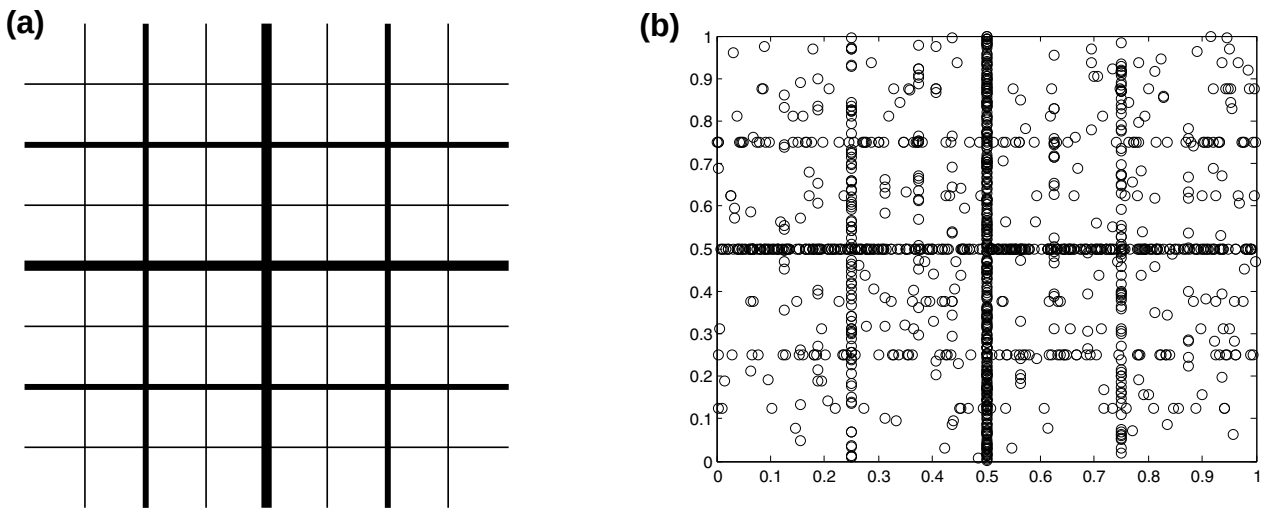

FIGURE 1 (a) Hyperfractal map support with $H = 3$; (b) hyperfractal with $H = 5$, $d_F = 3$, and $n = 1200$ nodes

$$d_r = 2\frac{\log(2/(1-p'))}{\log 2}.$$

3 | MAIN RESULTS

We recall the strong requirement that the vehicles should be covered in a proportion of $\gamma_{FC} > 99.99\%$. In an urban vehicular network supported by eMBB infrastructure, both modelled by hyperfractals, the authors of Ref. [35] have proven that under no constraints on the transmission range, the giant component tends to include all the nodes for n large.

In this analysis, under the constraint of a constant limited transmission range R_0, there will always be disconnected nodes and the number of gNBs to guarantee γ_{FC} would not be cost effective. Therefore, we dynamically deploy drones to extend the coverage of the gNBs by using hop-by-hop communications, as illustrated in Figure 2.

This should be done by considering the constraints in latency as well, which, in our model, translate to a maximum number of drones on which the packet is allowed to hop before reaching the gNB.

3.1 | Connectivity with fixed telecommunication infrastructure

The infrastructure location can be fitted to a hyperfractal distribution with dimension d_r and intensity ρ and provide a realistic model [32]. To demonstrate the need of drones and sake of reading, we first omit the existence of drones: a mobile node is covered only when a gNB exists at a distance lower than R_0. In this case, the following theorem gives the average number of nodes that are not in the coverage range of the infrastructure.

Theorem III.1 ***(Connectivity without drones)*** *Assuming n mobile nodes distributed according to a hyperfractal distribution of dimension d_F and a gNB distribution of dimension d_r and intensity ρ, if $\rho = n^\theta$ with $\theta > d_r/4$ then the average number of mobile nodes not covered by a gNB is nI_n with $I_n = O\left(n^{-\frac{(d_F-2)}{d_r}(2\theta - d_r/2)}\right)$.*

Remark 4 The quantity I_n is the probability that a mobile node is isolated and thus the theorem proves that the proportion of non-covered mobile nodes tends to zero.

Proof Let a mobile node be on a road of level H at the abscissa x. For the mobile node to be covered, it is necessary for a gNB to exist on the same street in the interval $[x - R_0, x + R_0]$.

We shall first estimate the probability $I_n(x, H)$ that a mobile node is not covered. Let $N_V(x)$ be the number of intersections of level V (*i.e.* with a street of level V) which are within distance R_0 of abscissa x on the road of level H. Since the placement of gNBs follows a Poisson process of mean $\rho p(H, V)$:

$$I_n(x,H) = \exp\left(-\rho\sum_V N_V(x)p(H,V)\right). \tag{3}$$

In order to get an upper bound $I_n(H)$ on $I_n(x, H)$ independent of the abscissa x, a lower bound of the quantities $N_V(x)$ is necessary. For any given integer $V \geq 0$, the intersections of level equal or larger than V are regularly spaced at frequency 2^{V+1} on the axis. Only half of them are exactly of level V, regularly spaced at a spatial frequency $2^V/L_n$ per metre (as a consequence of the construction process). Therefore, a lower bound of $N_V(x)$ is $\lfloor\frac{2^V R_0}{L_n}\rfloor$.

Let $q' = 1 - p'$ and V_n be the smallest integer, which satisfies $2^{V_n} \geq L_n/R_0$ (which is $\frac{L_1}{R_0}\sqrt{n}$). Therefore, the lower bound of $N_H(x)$ is 2^{V-V_n} when $V \geq V_n$ and 0 when $V < V_n$. Thus, the upper bound $I_n(H)$ of $I_n(x, H)$ is

$$I_n(H) = \exp\left(-\rho\sum_{V\geq V_n} 2^{V-V_n}p(H,V)\right)$$

with the expression $p(H, V) = (p')^2(q'/2)^{H+V}$ we get

$$I_n(H) = \exp\left(-\rho p'(q'/2)^{V_n+H}\right). \tag{4}$$

We now have $V_n \geq \log_2\frac{L_n}{R_0} = \log_2\frac{L_1}{R_0} + 1/2\log_2 n$; thus, $(q'/2)^{V_n} \leq \left(\frac{R_0}{L_1}\right)^{d_r/2} n^{-dr/4}$ and with $\rho = n^\theta$, we obtain $I_n(H) \leq \exp\left(-\left(\frac{R_0}{L_1}\right)^{d_r/2} n^{\theta-d_r/4}p'(q'/2)^H\right)$. From here, we can finish the proof since the proportion I_n of isolated mobile nodes is:

$$\begin{aligned} I_n &= 2\sum_H \lambda_H I_n(H) \\ &= \sum_H pq^H I_n(H) \\ &\leq \sum_H pq^H \exp\left(-\left(\frac{R_0}{L_1}\right)^{d_r/2} p'(q'/2)^H n^{\theta-d_r/4}\right) \end{aligned} \tag{5}$$

and we prove in the appendix (via a Mellin transform) that for any number $B > 0$

$$\sum_H pq^H \exp\left(-B(q'/2)^H y\right) = \frac{p(B)^{-\delta}}{\log(2/q')}\Gamma(\delta)y^{-\delta}(1 + o(1)) \tag{6}$$

for $y \to \infty$ with $\delta = \frac{d_F-2}{d_r/2}$. We complete the proof by using $y = n^{\theta-d_r/4}$. □

Let us now study the second regime of θ, $\theta < d_r/4$.

Theorem III.2 *For $\theta < d_r/4$, the proportion of covered mobile nodes tends to zero.*

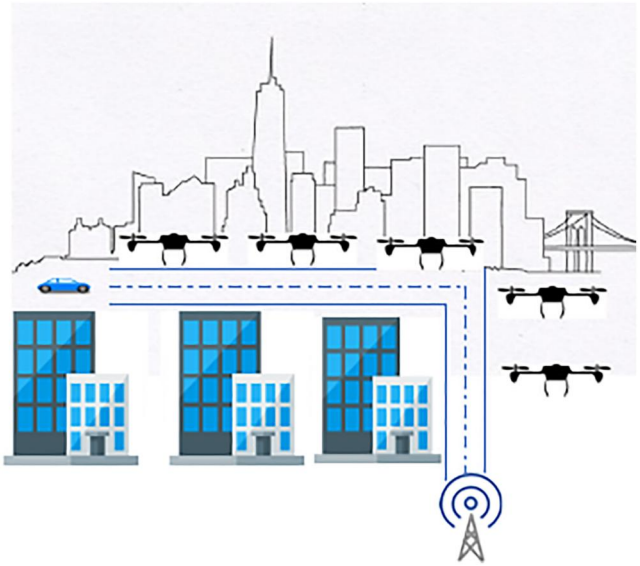

FIGURE 2 Extension of connectivity of vehicular networks using a moving network of flying drones to link to the fixed infrastructures

For u_i positive for all i, let $P(u_0, u_1, \ldots, u_V, \ldots) = E\left[\prod_V u_V^{N_V(x)}\right]$, the average being understood as random abscissa x uniformly distributed on the interval $[0, L_n]$.

Let $P_V(u_0, \ldots, u_{V-1})$ be a simplified notation of $P(u_0, \ldots, u_{V-1}, 1, 1, \ldots)$, that is, for all $i > V$, $u_i = 1$.

Lemma 1 *For all integer* V, $P_V(u_0, \ldots, u_{V-1}) \geq 1 - \frac{2^V R_0}{L_n}$.

Proof Naturally as the u_i are all positive, $P_V(u_0, u_1, \ldots, u_{V-1}) \geq P_V(0, \ldots, 0)$. The quantity $P_V(0, \ldots, 0)$ is the probability that for all $i < V$, $N_i(x) = 0$. This is equivalent to the fact that x is always at a distance larger than R_0 to any intersection of level higher than V. Since there are 2^V of such intersections, the measure of the union of all these intervals is smaller than $2^V R_0$; thus, the probability to have the abscissa x belonging to this union, thus having $N_i(x) = 0$ for all $i < V$, is smaller than this quantity divided by L_n. □

Lemma 2 *Assuming for all integer* i, $u_i \leq 1$, *for any integer* V_n *we have* $P(u_0, \ldots) \geq \prod_{V \geq V_n} u_V^{2^{V-V_n+1}} P_{V_n}(u_0, \ldots, u_{V_n-1})$.

Proof Indeed for $V \geq V_n$ we have $N_V(x) \leq 2^{V-V_n+1}$, thus

$$P(u_0, \ldots) \geq \prod_{V \geq V_n} u_V^{2^{V-V_n+1}} E\left[u_0^{N_0(x)} \cdots u_{V_n-1}^{N_{V_n-1}(x)}\right].$$

□

Let $V_n = \lceil \log_2 \frac{R_0}{L_n} \rceil$

Lemma 3 *Let* $V \leq V_n$, *the following holds*: $P_V(u_0, \ldots u_{V-1}) \geq u_{V-1} P_{V-1}(u_0, \ldots, u_{V-2})$.

Proof For $V < V_n$ we have $N_V(x) \leq 1$. Indeed the distance between two intersection with a street of level V are spaced by equal distance $L_n 2^{-V+1} > 2R_0$, thus for any arbitrary abscissa x the interval $[x - R_0, x + R_0]$ which span on a length $2R_0$ cannot contain more than one intersection of level V. □

Proof of theorem III.2. The following identity holds:

$$I_n(H) = P\left(e^{-\rho p(H,0)}, \ldots, e^{-\rho p(H,V)}, \ldots\right). \tag{7}$$

Clearly, with Lemma 2 we get

$$I_n(H) \geq \exp\left(-\rho \sum_{V \geq V_n} p(H, V) 2^{V-V_n+1}\right) \times P_{V_n}\left(e^{-\rho p(H,0)}, \ldots, e^{-\rho p(H,V_n-1)}\right).$$

Since $\theta < d_r/4$, the first right hand factor tends to one as the quantity $\sum_{V \geq V_n} \rho p(H, V) = O\left(\left(\frac{R_0}{L_1}\right)^{d_r/2} n^{\theta - d_r/4} p'(q'/2)^H\right)$ tends to zero.

Using lemma 3 the second term is lower bounded for any integer $k < V_n$ by:

$$\prod_{i=1}^{k} \exp(-\rho p(H, V_n - i)) \left(1 - 2^{V_n - k} \frac{R_0}{L_n}\right) \tag{8}$$

Each of the terms $\rho p(H, V_n - i) = O\left(n^{\theta - d_r/4} (q'/2)^{-i}\right)$ tends to zero; thus, $\exp(-\rho p(H, V - i))$ tends to 1. Since $2^{V_n} \leq 2L_n/R_0$, $1 - 2^{V_n - k} R_0/L_n \geq 1 - 2^{1-k}$. For any fixed k, we have $\liminf_n I_n(H) \geq 1 - 2^{1-k}$ uniformly in H. Since k can be made as large as possible, thus 2^{2-k} as small as we want, the $I_n(H)$ tends to 1 uniformly in H. □

3.2 | Extension of connectivity with drones

Now that we have analysed the connectivity properties of the network and observed the situation when nodes are not covered. We have discovered two regimes, in function of the existing gNB infrastructure features: $\theta > d_r/4$ and $\theta < d_r/4$. Let us provide the necessary dimensioning of the network in terms of UAVs for ensuring the required services for the first case. As in the second case the number of isolated nodes is overwhelming, we consider drones are not a desirable, cost-effective solution for connectivity. We have, therefore, also identified the regime for which drones are to be deployed.

Theorem III.3 *(Connectivity with drones)*
Assume n mobile nodes distributed according to a hyperfractal distribution of dimension d_F *and a gNB distribution of dimension* d_r *and intensity* ρ. *If* $\rho = n^\theta$ *with* $\theta > d_r/4$ *then the average number of drones needed to cover the mobile nodes not covered by gNBs is* $D_n = nI_n\left(1 + \sum_{k \geq 1} (k+1)^{2-d_F} \exp\left(-p'q'(R_0/L_1)^{d_r} n^{\theta - dr/2} k^{d_r}\right)\right)$.

Remark 5 when $d_F > 3$ and $\theta < d_r/2$ the distribution of the number of drones tends to be a power law of power $2 - d_F$.

When $\theta > d_r/2$ the average number of drones is asymptotically equivalent to the average number of isolated nodes. The probability that an isolated node needs more than one single drone decays exponentially.

Lemma 4 *Let $I_n(H, R)$ be an upper bound of the probability that an interval of length R on a road of level H does not contain any gNB. We have*

$$I_n(H,R) \le \exp\left(-\rho p'(q'/2)^H \left(\frac{R}{L_n}\right)^{d_r/2}\right). \tag{9}$$

Proof This is an adaptation of the estimate of $I_n(H)$ in the proof of theorem III.1, where we replace R_0 by R. Notice that $I_n(H) = I_n(H, R_0)$. □

Let us now look at the possibility of having gNBs at a Manhattan distance R. By Manhattan distance, we consider the path from one mobile node to a gNB is

- either the segment from the mobile node to the gNB if they are on the same road; in this case, the distance is the length of this segment and is called a *one leg* distance;
- or composed of the segment from the mobile node to the intersection to the road of the gNB and the segment from this intersection to the gNB; in this case, the distance is the sum of the lengths of the two segments and is called a *two-leg* distance.

Lemma 5 *Let $J_n(R)$ be the probability that a mobile node has no gNB at two-leg distance less than R, $J_n(R) \le \exp\left(-\rho p' q' \frac{(R/L_n)^{d_r}}{1+d_r/2}\right)$.*

Proof Let $J_n(H, R)$ be the probability that there is no relay on a road of level H at a two-leg distance smaller than R. From the mobile nodes the maximal gap to the next intersection of level H is $2^{-H+1}L_n$, we have

$$J_n(H,R) \le \prod_{i \le R2^H/L_n} \left(I_n\left(H, 2R - i2^{-H}L_n\right)\right)^2$$

Each factor $I_n(H, 2R - i2^{-H}L_n)$ comes from the fact that from the intersection of abscissa $i2^{1-H}L_n$ the two segments apart of the perpendicular road of length $R - i2^{1-H}L_n$ should not contain any relay. The power 2 comes from the fact that we have to consider two intersections apart at distance $i2^{1-H}L_n$ from the mobile node. We consider $H \ge H_R = \lceil \log_2 L_n/R \rceil$. For $H < H_R$ we will simply assume $J(H, R) \le 1$. For $H \ge H_R$ we have

$$J_n(H,R) \le \exp\left(-2\rho p'(q'/2)^H \sum_{i \le 2^H - H_R} \left(2R/L_n - i2^{-H}\right)^{d_r/2}\right)$$

with the fact that

$$\sum_{i=1}^{2^{H-H_R}} \left(2R/L_n - i2^{-H}\right)^{d_r/2} \ge 2^H \int_0^{2R/L_n - 2^{-H}} x^{dr/2} dx$$

$$= 2^H \frac{\left(2R/L_n - 2^{-H}\right)^{1+d_r/2}}{1+d_r/2}$$

$$\ge 2^H \frac{(R/L_n)^{1+d_r/2}}{1+d_r/2}$$

we obtain that

$$J_n(H,R) \le \exp\left(-\rho p'(q')^H \frac{(R/L_n)^{1+d_r/2}}{1+d_r/2}\right)$$

The overall evaluation of $J_n(R)$ is made of the product of all the $J(H, R)$ since the intersection and gNBs positions are independent:

$$J_n(R) = \prod_H J_n(H,R)$$

$$\le \exp\left(-\rho p' \sum_{H \ge H_R} (q')^H \frac{(R/L_n)^{1+d_r/2}}{1+d_r/2}\right)$$

$$= \exp\left(-\rho p'(q')^{H_R} \frac{(R/L_n)^{1+d_r/2}}{1+d_r/2}\right)$$

With the estimate that $(q')^{H_R} \ge q'(R/L_n)^{d_r/2-1}$ we get $J_n(R) \le \exp\left(-\rho p' q' \frac{(R/L_n)^{d_r}}{1+d_r/2}\right)$. □

Lemma 6 *Let $D(H, R)$ be the probability that for a mobile node on a road of level H there is no gNB at Manhattan distance less than R. We have $D(H, R) \le I_n(H, R)J_n(R)$. Let k be an integer and $P_n(H, k)$ be the probability that a mobile node on road of level H needs k or more drones to be connected to the closest gNB. We have*

$$P_n(H,k) \le I_n(H, kR_0)J_n((k-1)R_0) \tag{10}$$

Proof The fact that $D(H, R) \le I_n(H, R)J_n(R)$ comes from the fact that probability that there is no relay at distance R is equal to the product of the probabilities of the event: (i) there is no relay at one-leg distance smaller than R (this with probability smaller than $(I_n(H, R))$, (ii) there is no relay at a two-leg distance smaller than R (probability smaller than $J_n(R)$).
The expression for $P_n(H, k)$ comes from the fact that to have k or more drones we need no gNB within one-leg Manhattan distance kR_0 and no gNB within two-leg distance $(k-1)n$, for $k \ge 1$ since we have to lay an extra drone at road intersection. □

Proof of Theorem III.3. The average number of drones needed to connect mobile nodes on a road of level H to the closest gNB is $L_n(H) = \sum_{k \ge 1} P_n(H, k)$. Thus $L_n(H) \le I_n(H) + \sum_{k \ge 1} I_n(H, kR_0)J_n(kR_0)$

Therefore, the average total number D_n of drones is given by:

$$\begin{aligned} D_n &= n\sum_H \lambda_H \sum_{k\geq 1} P_n(H,k) \\ &\leq n\sum_H \lambda_H \sum_{k\geq 1} I_n(H,kR_0) J_n((k-1)R_0) \\ &\leq nI_n + \sum_{k\geq 1}\sum_H nI_n(H,(k+1)R_0) \\ &\times \exp\left(-\rho p' q' (kR_0/L_n)^{d_r}/(1+d_r/2)\right) \end{aligned}$$

By an adaptation of (6), we have $\sum_H \lambda_H I_n(H,(k+1)R_0) \sim (k+1)^{-\delta d_r/2} I_n$ and by the fact that with $\rho = n^\theta$ and $L_n = \sqrt{n}L_1$, $\rho(R_0/L_n)^{d_r} = (R_0/L_1)^{d_r} n^{\theta - d_r/2}$. Thus, we get the claimed result. □

Remark 6 The fact that the number of drones to connect the isolated mobile nodes is asymptotically equivalent to the number of isolated mobile nodes when $\theta > d_r/2$ is optimal when drone sharing is not allowed. We conjecture that the isolated mobile nodes are so dispersed that sharing the connectivity of a drone is unlikely. In the other case when $d_r/4 < \theta < d_r/2$ the number of drones per isolated node tends to be finite as soon as $d_F > 3$.

4 | GARAGES OF DRONES

While the fixed infrastructure is robust and can serve the vehicle requirements with a proper planning, the cost of installing and operating fixed infrastructure is substantial. In addition, as in many situations in telecommunications, the planning is often over-dimensioned in order to cope with 'worst case scenarios' (e.g. day vs. night traffic). In this sense, our scenario further offloads the traffic towards a flexible, 'ephemeral' infrastructure, advancing towards the so-called 'moving networks of drones'. We will now propose a procedure for trimming the number of required relays, by converting some into garages of drones, which will be dynamically deployed and launched to meet the requirements of the mobile users. The drones are to be seen as 'mobile relays', with the possibility to build chains of drones that will serve the user with hop-by-hop communication through a highly reconfigurable IAB.Although it has been envisioned for the drones to be shared between operators, it is unlikely this will be done in an early phase: each operator will own and maintain its own fleet of drones. Furthermore, as the UAVs are a cost effective and flexible solution for extending the coverage, the places for storing and charging them, what we call 'garages', are to be located in the same sites as the gNBs, owned by the operators.

We now provide a first straight-over insight on the home locations of the nomadic infrastructure.

We define as the '*flight-to-coverage*' time, the time necessary for a drone to leave the garage and be in a distance lower than R_0 to the UE and to the gNB, such as to be able to form the backhaul. In order to fulfil the service requirements, the flight-to-coverage time should be lower than the allowed delay. Again, the drone needs not to be hoovering over the UE or the gNB but just have them in the range of its Channel State Information Reference Signal beams.

We, thus, transform the flight-to-coverage time into constraints on connectivity (at all time), for a chain of drones of maximum length k. We want to select the relays that will be garages (and store drones) in order to minimise the number of garages and delay, that is, under the constraint that at most k hops are needed to forward the packets (and that the chains of drones are no longer than k).

We now describe informally an algorithm we use to select relays to become garages. Similar to a dominating set problem, we first make every relay a garage. We then check the garages in an arbitrary order $A_1, A_2, \ldots$. We then eliminate sequentially a garage if it has four relays at Manhattan distance less than R, one in each of the four quadrants, for example, as in Figure 3. We call these relays the 'covering' relays. They have the property that every mobile node at Manhattan distance smaller than R to the eliminated garage is necessary at Manhattan distance smaller than R to at least one of the covering relay. We call this property the covering transfer property.

Note that with the garage elimination heuristic, we eliminate the garage A_ℓ if it has a covering set made of four relays of index smaller than ℓ.

Lemma 7 *If a mobile node is at Manhattan distance smaller than R to at least one relay, then it is at Manhattan distance smaller than R to at least one non-eliminated garage.*

Proof Since there are no road with null density, the mobile node can be in any point of the map which is at Manhattan distance smaller than R from a relay. Let us suppose that there is such point X such that all relays at distance smaller than R are eliminated garage. Let i denote the smallest index among the indices of the relays at distance smaller than R. Since we suppose that its garage has been eliminated, the relay A_i is covered by four relays of smaller index. Let $j < i$ be the index of the covering relay, which is in the same quadrant of A_i as the point X. Since A_j and X are at Manhattan distance smaller than R of each other, this contradicts the fact that i is the smallest index of the relays

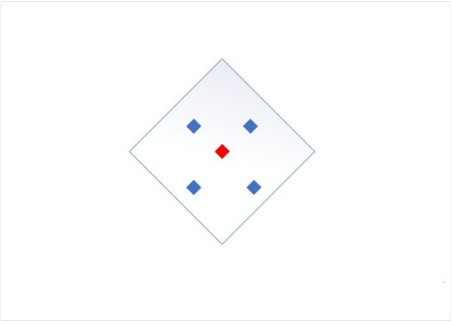

FIGURE 3 Garage elimination algorithm: selection of garages (red) with four garages within Manhattan distance R (blue)

within distance R from X. Therefore, X has necessarily at least one non-eliminated garage within distance R. □

Consequently, we will eliminate quickly all relays, which have themselves a neighbouring relay in distance of less than R; therefore, there is no uncovered segment of road between the two relays. The remaining garages should hold drones to ensure connectivity within the delay tolerated.

Figure 4 illustrates an operating model scenario with a garage of drones. A garage selected on a relay at an intersection of level (H, V) should be able to send its drones to all the cars arriving from the closest relays, forming together chains of drones of maximum length k. A chain of drones will be constructed with drones coming from both of the neighbouring garages, as the passing of a car through a relay is announced to the neighbouring relay through the wired F1 interface such that the following garage in the direction of movement can send its drones to meet the car to ensure the coverage along the path.

A garage should be able to hold enough drones to ensure the continuity of service for all upcoming vehicles on the lines of the hyperfractal support crossing the area where the drones can move in an acceptable time. Note that as the arriving traffic flow in the 'cell' served by the garage is a mixture of Poisson point processes on lines, the average incoming traffic the garage is serving can be computed, given the distance towards the neighbouring relays.

We assume that the average speed of a drone is considered to be comparable to the maximum speed of a car. The drones of a garage can, thus, be in three possible states: *in route* towards the car they will be serving, *serving* a car, and *coming back* from the service.

Consequently, this procedure leads to the property that within the 'cell' around a garage, the graph is connected over time using the drones (as per Figure 4). We will refer to this cell as a 'moving network of drones'.

5 | NUMERICAL EVALUATIONS

In this section, we first provide some simulations on the connectivity of gNBs, UEs and drones. We, then, provide some simulations on the garage locations and their properties.

The numerical evaluations are run in a locally built simulator in MatLab, following the description provided in Section 2 for both the stochastic modelling of the location of the entities and the communication model. The map length is of one unit and a scaling is performed in order to respect the scaling of real cities as well as communication parameters.

5.1 | Connectivity of gNBs, UEs and drones

We first give some visual insight on the connectivity variation with the fractal dimension of the gNBs and θ. Figure 5a shows in red * the locations of vehicular UEs for $n = 400$ and $d_F = 3$ and in black circles the locations of the gNBs for $d_r = 3$ and $\rho = n^\theta$ with $\theta = 1$. We are, therefore, in the first regime of θ, $\theta > d_r/4$. On the other hand, Figure 5b displays a snapshot of a network for the same d_F, d_r and n, the second regime of θ, with $\theta < d_r/4$, as more precisely $\theta = 1/2$.

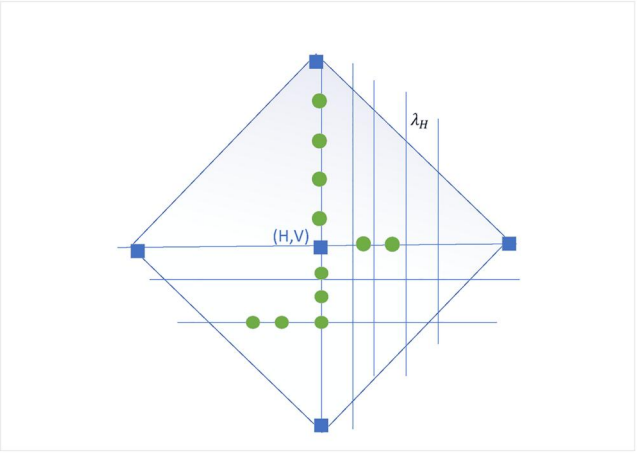

FIGURE 4 Garage operating model: allowing to cover any uncovered vehicle with a chain of at most k drones

Notice how the number of gNB falls drastically for the second regime of θ. This generates, as expected and graphically visible in Figure 6, numerous disconnected UEs. For this regime, the number of isolated UEs is overwhelming, as clearly shown in Figure 6b.

We now look at what happens for a higher fractal dimension of the fixed telecommunication infrastructures. Figure 7a shows a snapshot of a network with $n = 400$ vehicular UEs (in red *) and $d_F = 3$ and gNBs with $d_r = 5.5$ and $\rho = n^\theta$ with $\theta = 1$ (in black circles), while Figure 7b displays, for the same d_F, d_r and n, but $\theta = 1/2$. In both cases, we are in the regime $\theta < d_r/4$.

Similarly to Figure 6, Figure 8 shows a snapshot of the isolated UEs for the two regimes of θ for $d_r = 5.5$. Notice that the number of isolated nodes is significantly higher for a large fractal dimension of the eMBB infrastructure, even for the first regime of θ.

Let us now look at the validation of Theorem III.1 on the number of isolated nodes; this is an important parameter estimation as it gives the operator insight on the requirements for dimensioning the network. Figure 9 shows the proportion of UEs that are not covered by a gNB when we vary the total number of devices and for two values of the fractal dimension of the gNBs: $d_r = 3$ and $d_r = 4$. In both cases, the fractal dimension of the nodes is $d_F = 3$ and $n = \rho$, therefore $\theta = 1$.

Notice that we used the expression in (5) for a tighter bound or the expression in (6) in Theorem III.1.

Next, for three values of fractal dimension of gNBS, $d_r = 3$, $d_r = 4$ and $d_r = 5$ respectively, yet for a case of $\theta = 1/2$, we show in Figure 10, that the number of isolated nodes tends to the actual number of nodes in the network, as stated in Theorem III.2.

This confirms again that in the case when $\theta < d_r/4$, the eMBB infrastructure alone cannot provide the required connectivity and consequently the number of disconnected nodes is overwhelming.

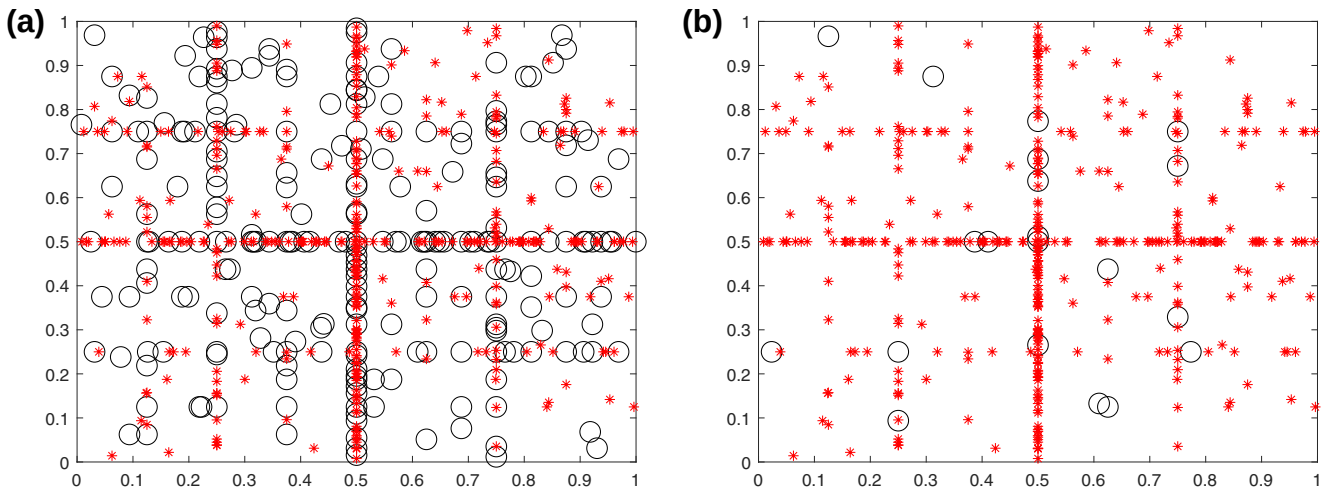

FIGURE 5 UEs and gNBs, $d_F = 3$, $d_r = 3$, and $n = 400$. (a) $\theta > d_r/4$. (b) $\theta < d_r/4$

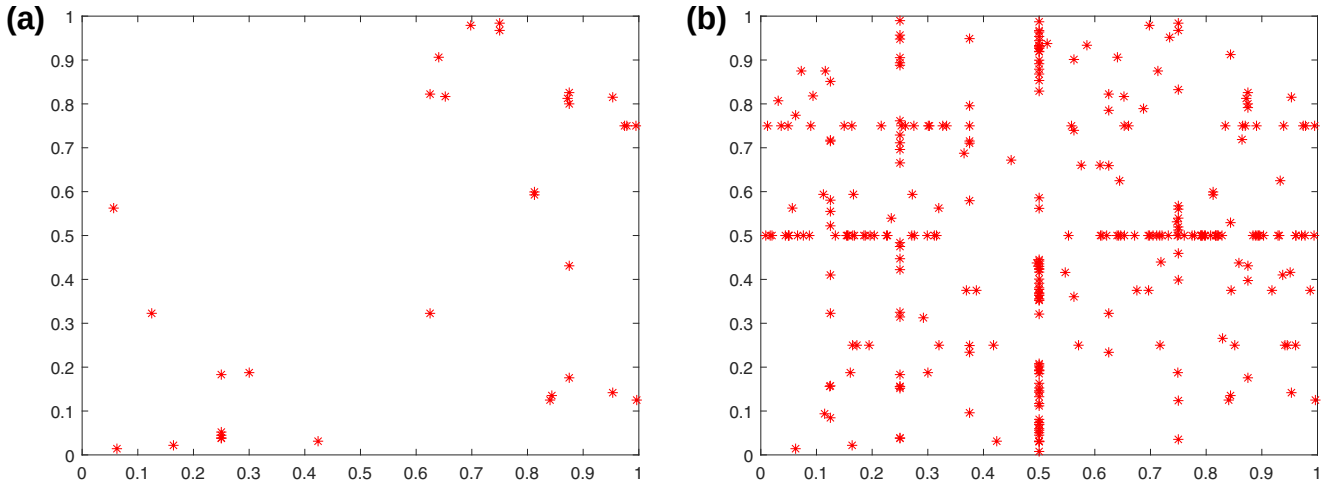

FIGURE 6 Snapshot of user equipments (UEs) not covered, $d_F = 3$, and $d_r = 3$. (a) $\theta > d_r/4$. (b) $\theta < d_r/4$

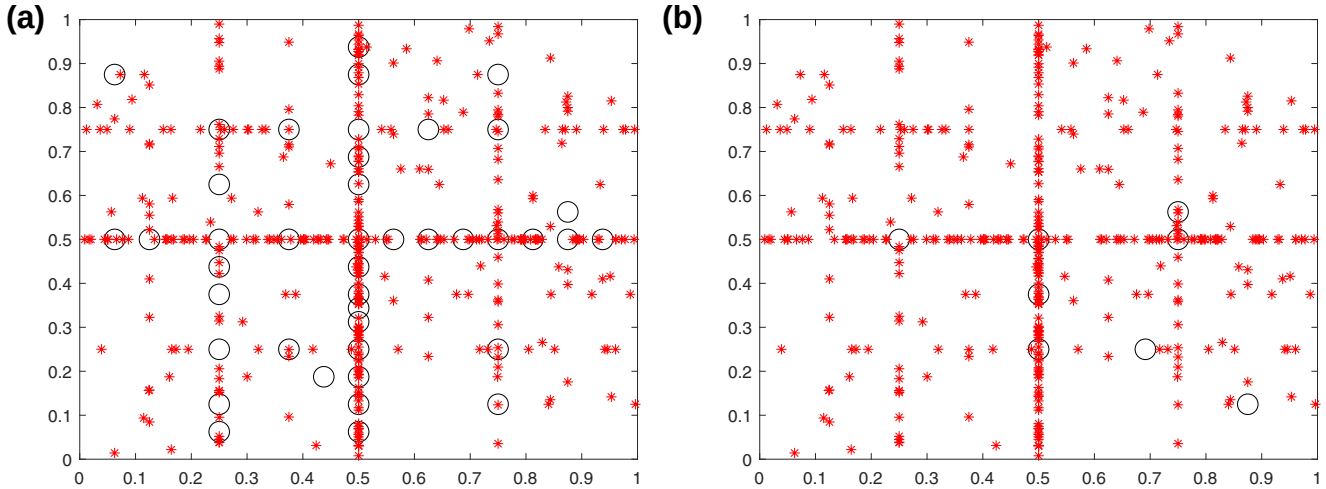

FIGURE 7 UEs and gNBs, $d_F = 3$, $d_r = 5.5$, and $n = 400$. (a) $\theta = 1$. (b) $\theta = 1/2$

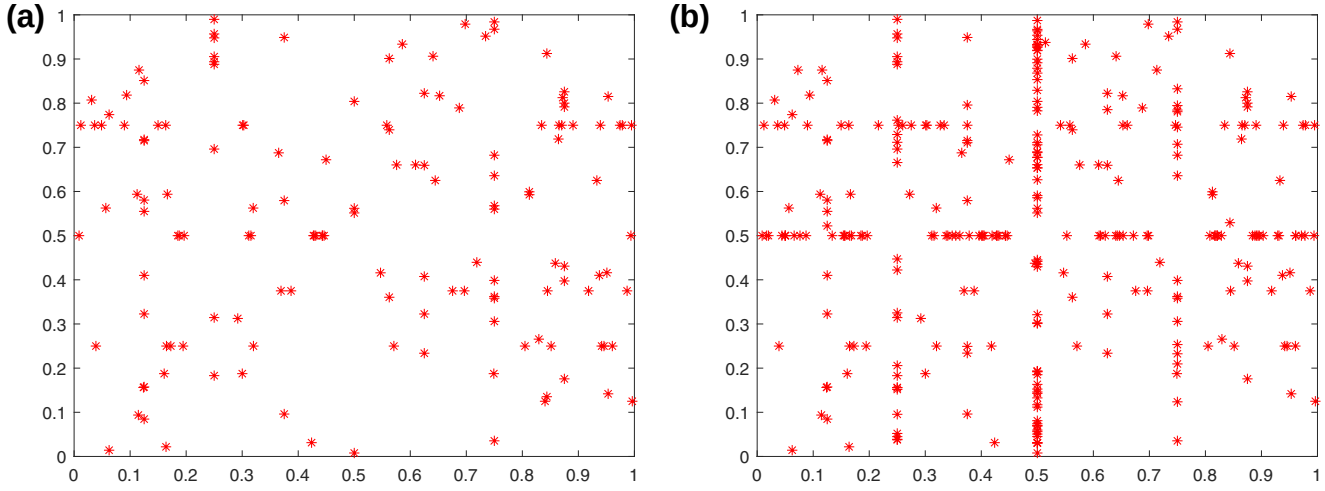

FIGURE 8 Snapshot of user equipments (UEs) not covered, $d_F = 3$, and $d_r = 5.5$. (a) $\theta > d_r/4$. (b) $\theta < d_r/4$

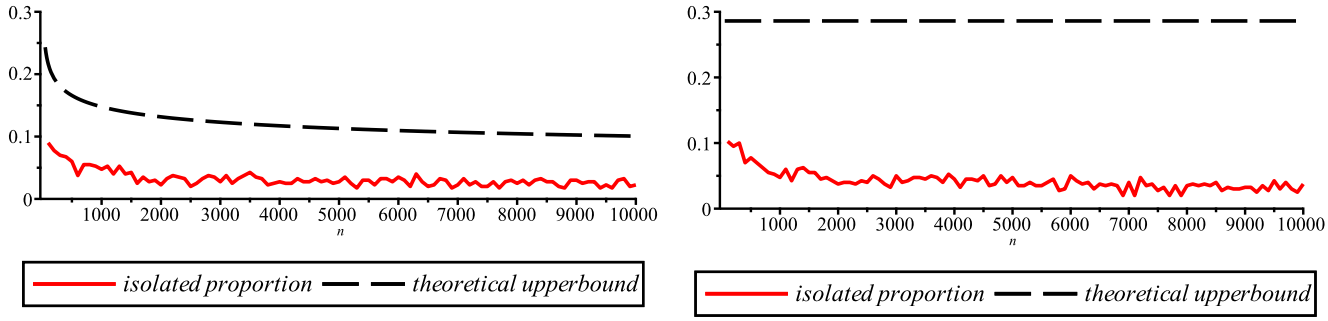

FIGURE 9 (left) $d_r = 3$ and $d_F = 3$; (right) $d_r = 4$ and $d_F = 3$

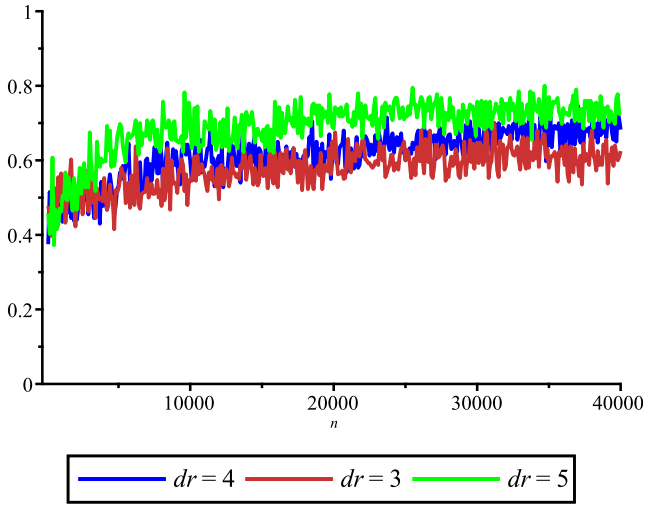

FIGURE 10 Proportion of isolated nodes for $\theta < d_r/4$

Figure 11 illustrates the result proved in Theorem III.3: the number of drones required to ensure connectivity for the isolated UEs (when $\theta > d_r/4$) behaves asymptotically like the number of isolated nodes. Indeed in the figure the features are indistinguishable.

5.2 | Location and size of drone garages

We run some simulations in order to validate the physical distance requirements between mobile nodes, relays and garages. In order to have realistic figures, we have assumed that the practical range of emission with mmWave is of order 100 m, and that the density of mobile nodes is around 1000 per square kilometre. This would lead to $L_1 = \sqrt{1000}$ m, equivalent to a square of 1 square kilometre, has a side length of 10 times the radio range and contains 1000 mobile nodes. We fix $d_F = 3$ and $d_r \approx 2.3$ (with $p_r = 0.1$).

We first compute the distribution of the distance of the mobile nodes to their closest base stations expressed in hop count in Figure 12. A hop count of one means that the mobile nodes is in direct range to a base station. A hop count of k (k integer) means that the mobile nodes would need $k-1$ drones to let it connected to its closest base station. We display the distribution for various values of n (green: $n = 5,000$; blue: $n = 10,000$; red: $n = 20,000$; brown: $n = 40,000$; black $n = 80,000$).

Second, in Figure 13, we compute the average number of isolated nodes (in blue) (*i.e.* the mobile nodes not at a direct range to a base station) and at the same time the average number of drones (in brown) to connect them to the closest base station. The two numbers are given as a fraction of the total number of mobile nodes present in the map.

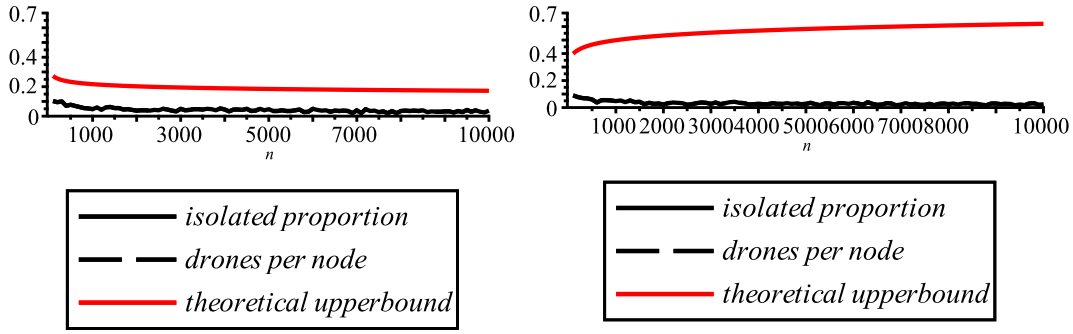

FIGURE 11 Number of drones for connectivity (left) $d_r = 3$ and $d_F = 3$; (right) $d_r = 4$ and $d_F = 3$

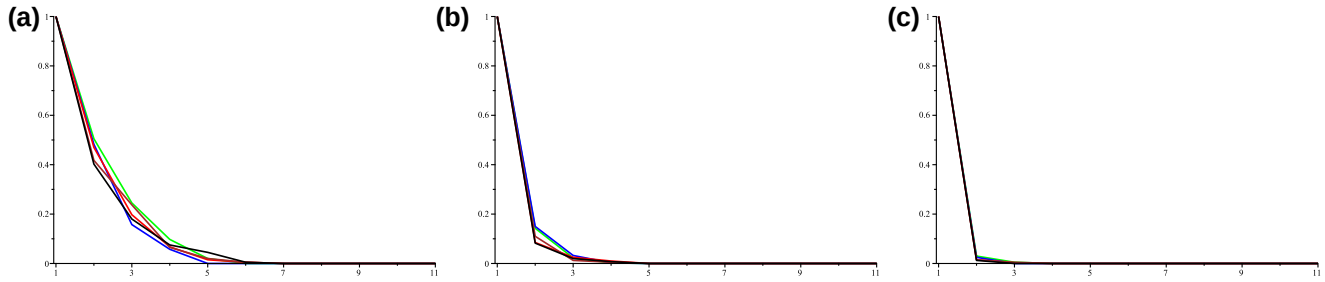

FIGURE 12 Distribution of distance to base stations in hop count. (a) $\theta = d_r/4$. (b) $\theta = 1.2d_r/4$. (c) $\theta = 1.4d_r/4$

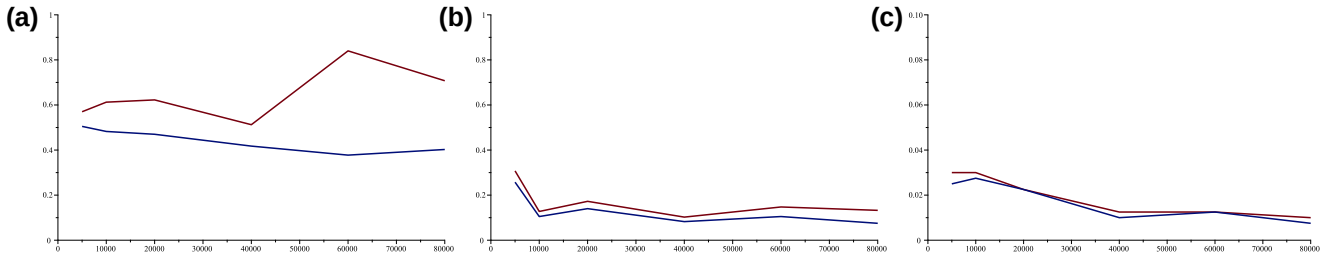

FIGURE 13 Proportion of isolated nodes (blue), proportion of drones (brown), versus the total number n of mobile nodes. (a) $\theta = d_r/4$. (b) $\theta = 1.2d_r/4$. (c) $\theta = 1.4d_r/4$ (notice the change of scale)

In Figure 14, we display the map of the garage locations after reduction on base stations. The reduction is made according to various coverage radii (the parameter R, respectively) which vary from radio ranges 5 (500 m) to 80 (8 km). We can see as expected that the garage density decreases when the coverage radius increases. The parameters are $n = 50,000$ and $\theta = 1.2\frac{d_r}{4}$. The coverage radius impacts the delay at which the drones can move to new mobile nodes, although many of these moves could be easily predicted from the aim and trajectory of the mobile nodes. Figure 15 shows the variation of size of the garage set as function of the coverage radius. The parameters are $n = 50,000$; in brown, $\theta = d_r/4$; in blue, $\theta = 1.2d_r/4$; and in green, $\theta = 1.4d_r/4$. When the coverage radius is zero, every relay is a garage and we get the initial number of relays. We notice that when the coverage radius tends to infinity, the limit density of garages is not bounded and increases with the number of relays. We conjecture that it increases as the logarithm of this number. On the right subfigure, we display the size of the garage set when the city map is considered on a torus without border. In this case the garage size decreases to 1 when the coverage radius increases. Figure 16 gives examples of garage maps in a torus.

Figure 17 shows the distribution of distance of the mobile nodes to the closest garage. Green is for coverage radius $5R_n$, blue for coverage radius $10R_n$, red for $20R_n$, brown for $40R_n$, and black for $80R_n$. We notice that despite the coverage radius increases the typical distance to the closest garage does not grow too much in comparison because the residual density of garage prevents that. Remember that the distance to the closest garage is larger than the number of drones needed to connect the mobile node to the closest relay, which is given by Figure 12. The distance to the closest garage gives an indication on how fast drones can be moved towards new mobile nodes.

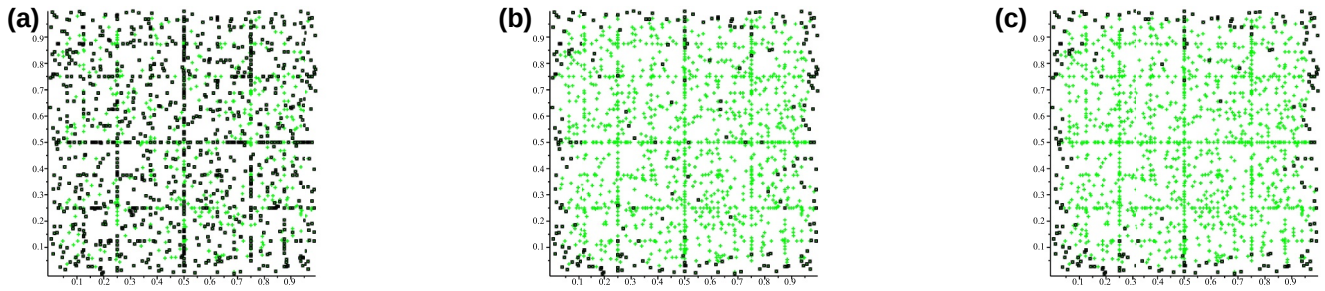

FIGURE 14 Map of drone garages (black circles), among the base stations (green crosses), for different coverage distances; (a) coverage distance $5R_n$, (b) coverage distance $20R_n$ and (c) coverage distance $80R_n$

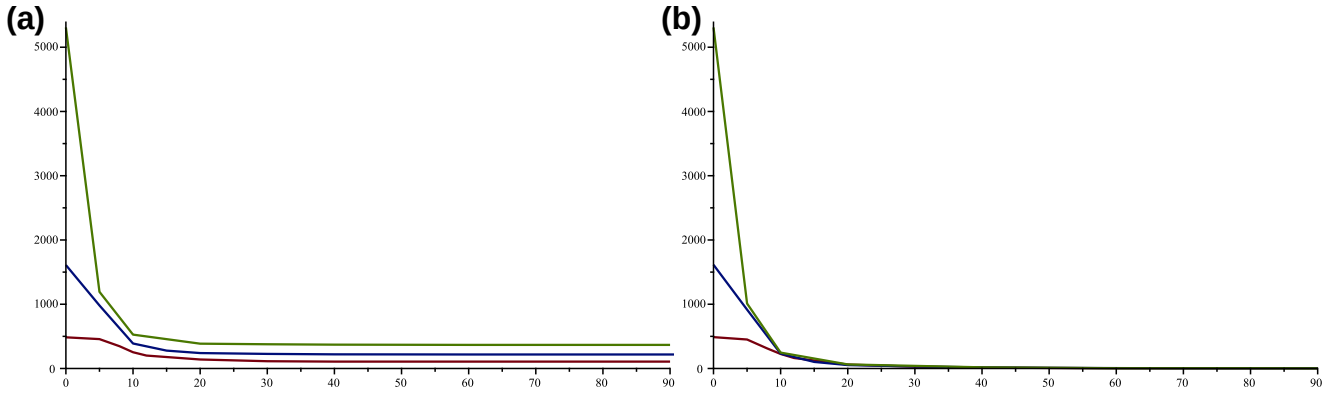

FIGURE 15 Size of the garage set as function of coverage radius, in brown $\theta = d_r/4$, in blue $\theta = 1.2d_r/4$, and in green $\theta = 1.4d_r/4$. (a) Garage number in a map with border. (b) In a torus map with no border

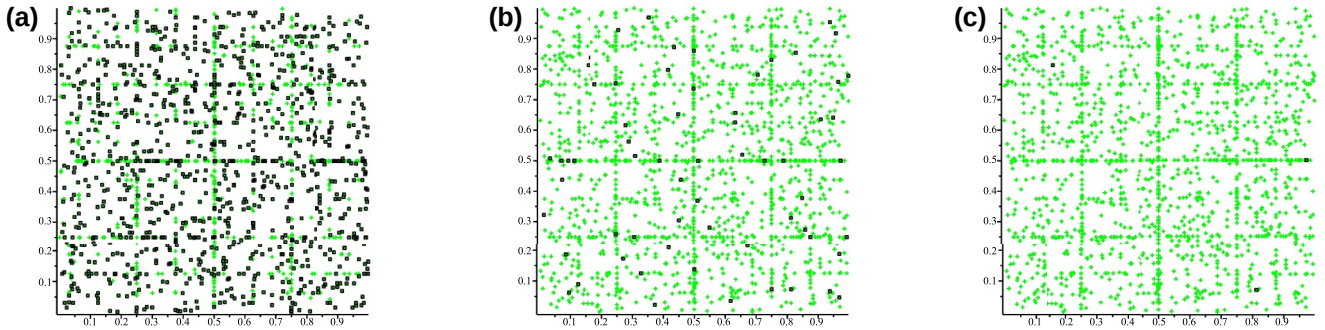

FIGURE 16 Map of drone garages (black circles), among the base stations (green crosses), for different coverage distances in a torus map; (a) coverage distance $5R_n$, (b) coverage distance $20R_n$ and (c) coverage distance $80R_n$

6 | CONCLUSIONS

This work has provided a study of the connectivity properties and dimensioning of the moving networks of drones used as a flying backhaul in an urban environment with vehicular users.

By making use of the hyperfractal model for both the vehicular networks and for the fixed eMBB infrastructures, we have derived analytic bounds on the requirements in terms of connectivity extension: we have proved that for n mobile nodes (distributed according to a hyperfractal distribution of dimension d_F) and an average of ρ gNBs (of dimension d_r) if $\rho = n^{\theta}$ with $\theta > d_r/4$, the average fraction of mobile nodes not covered by a gNB tends to zero such as $O\left(n^{-\frac{(d_F-2)}{d_r}\left(2\theta-\frac{d_r}{2}\right)}\right)$. Furthermore, for the same regime of θ, we have obtained that the number of drones to connect the isolated mobile nodes is asymptotically equivalent to the number of isolated mobile nodes. This gives insights on the dimensioning of the flying backhauls and also limitations of the usage of UAVs (second regime of θ). This work has also initiated the discussions on the placement of the home locations of the drones, what we called the 'garage of drones'. We have provided a fast procedure to select the relays that will be garages (and store drones) in order to minimise the number of garages and minimise the delay.

Our simulation results concur with our bounds and illustrate the step-change of regime based on θ. Our simulations also show how this can be exploited to have as few garages as possible, while having drones servicing efficiently the mobile

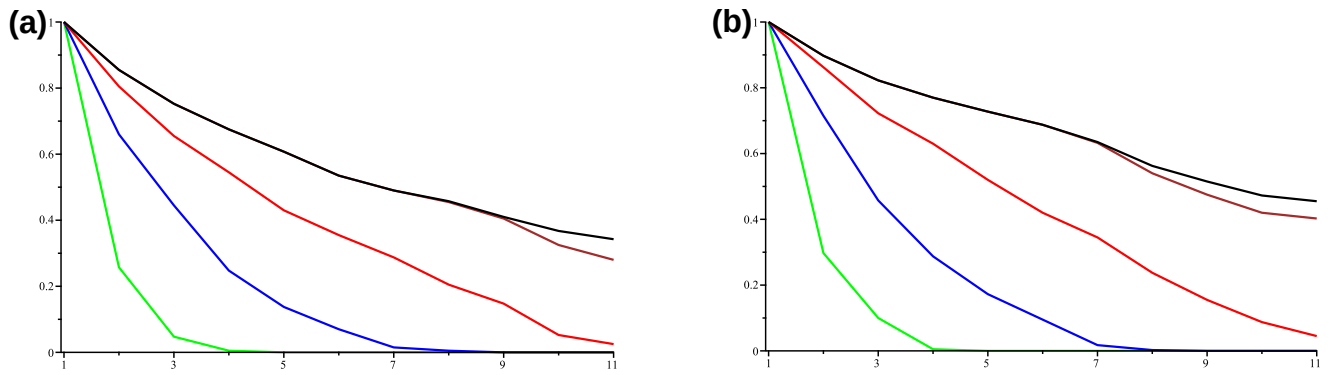

FIGURE 17 Distribution of distances to closest garage (in hop count) for various coverage radii. (a) $n = 50,000$ and $\theta = 1.2d_r/4$. (b) $n = 50,000$ and $\theta = 1.4d_r/4$

vehicles with limited delay, hence making the scenario attractive for further study and possible implementation.

Overall our results have provided a realistic stochastic communication model for studying the development of 5G in smart cities. The interest of such an innovative framework was demonstrated by the computation of exact bounds and the identification of particular behaviours (such as the characterisation of a threshold). It is also a step towards constructing a smart city modelling framework that can be exploited in other urban scenarios.

ACKNOWLEDGEMENTS

Part of this work was presented at WiSARN'2020, IEEE Conference on Computer Communications Workshops (INFOCOM WKSHPS), International Workshop on Wireless Sensor, Robot and UAV Networks, July 6th, 2020, (Online). Connecting flying backhauls of drones to enhance vehicular networks with fixed 5G NR infrastructure, P. Jacquet D. Popescu and B. Mans, IEEE Press, pp. 472–477, doi10.1109/INFOCOMWKSHPS50562.2020.9162670. B. Mans was supported in part by the Australian Research Council under Grant DP170102794.

CONFLICT OF INTEREST

The author declares that there is no conflict of interest that could be perceived as prejudicing the impartiality of the research reported.

DATA AVAILABILITY STATEMENT

The data that support the findings of this study are available on request from the corresponding author.

ORCID

Bernard Mans https://orcid.org/0000-0001-7897-2043

REFERENCES

1. Gall, Q.L., et al.: Relay-assisted device-to-device networks: connectivity and uberization opportunities. In: 2020 IEEE Wireless Communications and Networking Conference (WCNC), pp. 1–7 (2020)
2. Alzahrani, B.A., et al.: UAV assistance paradigm: state-of-the-art in applications and challenges. J. Netw. Comput. Appl. 166, 102706 (2020). https://doi.org/10.1016/j.jnca.2020.102706
3. Popescu, D., et al.: Information dissemination speed in delay tolerant urban vehicular networks in a hyperfractal setting. IEEE/ACM Trans. Netw. 27(5), 1901–1914 (2019). https://doi.org/10.1109/tnet.2019.2936636
4. Gupta, L., Jain, R., Vaszkun, G.: Survey of important issues in UAV communication networks. IEEE Communications Surveys & Tutorials. 18(2), 1123–1152 (2016). https://doi.org/10.1109/comst.2015.2495297
5. Minoli, D., Sohraby, K., Occhiogrosso, B.: Iot considerations, requirements, and architectures for smart buildings—energy optimization and next-generation building management systems. IEEE Internet Things J. 4(1), 269–283 (2017). https://doi.org/10.1109/jiot.2017.2647881
6. Wang, J., et al.: Taking drones to the next level: cooperative distributed unmanned-aerial-vehicular networks for small and mini drones. IEEE Veh. Technol. Mag. 12(3), 73–82 (2017). https://doi.org/10.1109/mvt.2016.2645481
7. Wang, J., et al.: Vehicular sensing networks in a smart city: principles, technologies and applications. IEEE Wireless Commun. 25(1), 122–132 (2018). https://doi.org/10.1109/mwc.2017.1600275
8. Zeng, Y., Wu, Q., Zhang, R.: Accessing from the sky: a tutorial on UAV communications for 5G and beyond. Proc. IEEE. 107(12), 2327–2375 (2019). https://doi.org/10.1109/jproc.2019.2952892
9. Mozaffari, M., et al.: A tutorial on uavs for wireless networks: applications, challenges, and open problems. IEEE Communications Surveys Tutorials. 21(3), 2334–2360 (2019). https://doi.org/10.1109/comst.2019.2902862
10. Wu, Q., Zeng, Y., Zhang, R.: Joint trajectory and communication design for multi-UAV enabled wireless networks. IEEE Trans. Wireless Commun. 17(3), 2109–2121 (2018). https://doi.org/10.1109/twc.2017.2789293
11. Oubbati, O.S., et al.: Dispatch of uavs for urban vehicular networks: a deep reinforcement learning approach. IEEE Trans. Veh. Technol. 70(12), 13174–13189 (2021). https://doi.org/10.1109/tvt.2021.3119070
12. Zeng, Y., Zhang, R., Lim, T.J.: Wireless communications with unmanned aerial vehicles: opportunities and challenges. IEEE Commun. Mag. 54(5), 36–42 (2016). https://doi.org/10.1109/mcom.2016.7470933
13. 5G Self Backhaul- Integrated Access and Backhaul,. http://www.techplayon.com/5g-self-backhaul-integrated-access-and-backhaul/. Accessed 19 July 2019
14. Seliem, H., et al.: Delay analysis for drone-based vehicular ad-hoc networks. In: 2017 IEEE 28th Annual International Symposium on Personal, Indoor, and Mobile Radio Communications (PIMRC), pp. 1–7 (2017)
15. Sekander, S., Tabassum, H., Hossain, E.: Multi-tier drone architecture for 5G/B5G cellular networks: challenges, trends, and prospects. IEEE Commun. Mag. 56(3), 96–103 (2018). https://doi.org/10.1109/mcom.2018.1700666
16. Kalantari, E., et al.: Backhaul-aware robust 3D drone placement in 5G+ wireless networks. In: 2017 IEEE International Conference on Communications Workshops (ICC Workshops), pp. 109–114 (2017)

17. Kalantari, E., Yanikomeroglu, H., Yongacoglu, A.: On the number and 3d placement of drone base stations in wireless cellular networks. In: 2016 IEEE 84th Vehicular Technology Conference (VTC-Fall), pp. 1–6 (2016)
18. Seliem, H., et al.: Drone-based highway-VANET and DAS service. IEEE Access. 6, 20125–20137 (2018). https://doi.org/10.1109/access.2018.2824839
19. Seliem, H., et al.: Delay analysis for drone-based vehicular ad-hoc networks. In: 2017 IEEE 28th Annual International Symposium on Personal, Indoor, and Mobile Radio Communications (PIMRC), pp. 1–7 (2017)
20. Mignardi, S., Verdone, R.: On the performance improvement of a cellular network supported by an unmanned aerial base station. In: 2017 29th International Teletraffic Congress (ITC 29), vol. 2, pp. 7–12 (2017)
21. Majd, A., et al.: Integrating learning, optimization, and prediction for efficient navigation of swarms of drones. In: 2018 26th Euromicro International Conference on Parallel, Distributed and Network-Based Processing (PDP), pp. 101–108 (2018)
22. Besada, J.A., et al.: Drones-as-a-service: a management architecture to provide mission planning, resource brokerage and operation support for fleets of drones. In: 2019 IEEE International Conference on Pervasive Computing and Communications Workshops (PerCom Workshops), pp. 931–936 (2019)
23. Union, I.T.: Minimum Requirements Related to Technical Performance for IMT-2020 Radio Interface(s). https://www.itu.int/pub/R-REP-M.2410-2017
24. OECD: Metropolitan areas. [Online]. https://www.oecd-ilibrary.org/content/data/data-00531-en
25. Bertaud, A.: The spatial organization of cities: deliberate outcome or unforeseen consequence? Working Paper 2004,01, 2004. [Online]. http://hdl.handle.net/10419/23612
26. EMTA: Towards a Sustainable Mobility in the European Metropolitan Areas (2000). [Online]. https://www.emta.com/IMG/pdf/report_mobility.pdf?23/27f75199660419ee3d68e55391fdba90e900ae67
27. Batty, M., Longley, P.: Fractal Cities. Academic U.K. (1994)
28. Batty, M.: Cities and Complexity: Understanding Cities with Cellular Automata, Agent-Based Models, and Fractals. The MIT press (2005)
29. Batty, M.: The size, scale, and shape of cities. Science. 319(5864), 769–771 (2008). https://doi.org/10.1126/science.1151419
30. Batty, M.: Digital twins. Environment and Planning B: Urban Analytics and City Science. 45(5), 817–820 (2018). https://doi.org/10.1177/2399808318796416
31. Jacquet, P., Popescu, D., Mans, B.: Broadcast speedup in vehicular networks via information teleportation. In: 2018 IEEE 43rd Conference on Local Computer Networks (LCN), pp. 369–376 (2018)
32. Jacquet, P., Popescu, D., Mans, B.: Energy trade-offs for end-to-end communications in urban vehicular networks exploiting an hyperfractal model. In: MSWIM DIVANet 2018 (2018)
33. Mandelbrot, B.B.: The Fractal Geometry of Nature. W. H. Freeman (1983)
34. Jacquet, P., Popescu, D.: Self-similarity in Urban Wireless Networks: Hyperfractals. In: Workshop on Spatial Stochastic Models for Wireless Networks. SpaSWiN (2017)
35. Jacquet, P., Popescu, D.: Self-similar Geometry for Ad-Hoc Wireless Networks: Hyperfractals. In: 3rd Conference on Geometric Science of Information. Société Mathématique de France (2017)
36. Flajolet, P., Gourdon, X., Dumas, P.: Mellin transforms and asymptotics: harmonic sums. Theor. Comput. Sci. 144(1-2), 3–58 (1995). https://doi.org/10.1016/0304-3975(95)00002-e

How to cite this article: Popescu, D., Jacquet, P., Mans, B.: Connecting flying backhauls of unmanned aerial vehicles to enhance vehicular networks with fixed 5G NR infrastructure. IET Smart Cities. 4(4), 239–254 (2022). https://doi.org/10.1049/smc2.12034

APPENDIX

Proof that $f(y) = \sum_H pq^H \exp\left(-B(q'/2)^H y\right) = \frac{p(p')^{-\delta}}{\log(2/q')}\Gamma(\delta)\, y^{-\delta}(1 + o(1))$. We use the technique in Ref. [36] by the Mellin transform $f^*(s) = \int_0^\infty f(y) y^{s-1} dy$, which is defined for some complex number s such that $\Re(s) > 0$. Indeed since the Mellin transform of $\exp(-B(q'/2)^H y)$ is $\left(B(q'/2)^H\right)^s \Gamma(s)$ where $\Gamma(s)$ is the Euler 'Gamma' function defined for $\Re(s) > 0$, thus, $f^*(s) = \sum_H pq^H \left(B(q'/2)^H\right)^{-s} \Gamma(s) = \frac{pB^{-s}}{1-q(q'/2)^{-s}}\Gamma(s)$ as long as $\Re(s) < \delta$ (thus the sum $\sum_H pq^H \left(B(q'/2)^H\right)^{-s}$ absolutely converges).

The asymptotic of function $f(y)$ is obtained by the inverse Mellin transform as explained in Ref. [36] as the residues of function of $f^*(s)y^{-s}$ on the main pole $s = \delta$ which lead to the claimed asymptotic expression. To the risk of being pedantic the Ref. [36] also mentions that there are additional poles on the complex numbers $\delta + 2ik\pi/\log(q'/2)$ for k integer which lead to negligible fluctuations of the main asymptotic term.